LIMITING EFFECTS IN THE TRANSVERSE-TO-LONGITUDINAL EMITTANCE EXCHANGE TECHNIQUE FOR LOW ENERGY RELATIVISTIC ELECTRON BEAMS*

M. M. Rihaoui[1,2], P. Piot[1,3], J. G. Power[2] and W. Gai[2]
[1] Department of Physics, Northern Illinois University DeKalb, IL 60115
[2] High Energy Physics Division, Argonne National Laboratory, Argonne, IL 60439, USA
[3] Accelerator Physics Center, Fermi National Accelerator Laboratory, Batavia, IL 60510, USA

Abstract

Transverse to longitudinal phase space manipulation hold great promises, e.g., as a potential technique for repartitioning the emittances of a beam. A proof-of-principle experiment to demonstrate the exchange of a low longitudinal emittance with a larger transverse emittance is in preparation at the Argonne Wakefield Accelerator using a $\sim$ 12 MeV electron beam. In this paper we explore the limiting effects of this phase space manipulation method including high order and collective effects. A realistic start-to-end simulation of the planned proof-of-principle experiment including sensitivity studies is also presented.

INTRODUCTION

Many advanced acceleration and light source concepts rely on the production of bright electron beams which often rely on phase space manipulations within one or two degrees of freedom. These manipulations are necessary to tailor the phase space distribution for a specific front-end application. In some cases the front-end applications require an emittance partition different from the emittance partition produced by the electron. It is therefore advantageous and sometime necessary to repartition the six-dimensional phase space to individually match the desired two-dimensional phase spaces.

The emittance exchange concept was first discussed in the context of B-factory [1] as a way to achieve very small β^* value at the interaction point. The scheme was later explored as a possible alternative for mitigating microbunching instability in electron beams [2] or for improving the performance of single-pass FELs [3]. There are several solutions capable of performing this transverse-to-longitudinal phase space exchange [4]. A possible beamline capable of swapping the horizontal (x, x') and longitudinal (z, δ) phase spaces, consists of a horizontally-deflecting cavity, operating on the TM_{110}-like mode, flanked by two identical horizontally-dispersive sections henceforth referred to as "dogleg."

* The work of M.R. and P.P. was supported by the US Department of Energy under Contract DE-FG02-08ER41532 with Northern Illinois University. W.G., and J.P., are supported by the U.S. Department of Energy under Contract No. DE-AC02-06CH11357 with Argonne National Laboratory.

PROOF-OF-PRINCIPLE EXPERIMENT

The proof-of-principle experiment, currently under preparation at the Argonne Wakefield Accelerator (AWA) [5] incorporates an emittance exchange beamline similar to the one described in the previous section; see Fig. 1.

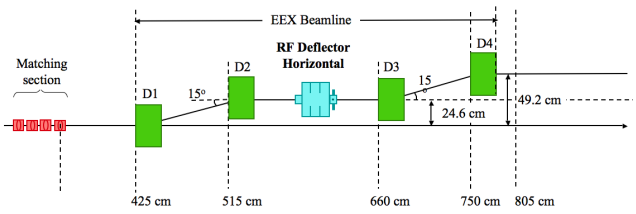

Figure 1: Schematics of the AWA emittance exchange experiment. Green rectangles are to dipoles and red ones to quadupoles. The positions are w.r.t. the photocathode.

The deflecting cavity is a 1.3 GHz normal conducting 1/2-1-1/2 cell structure optimized to minimize the beam offset [6]. Although the cavity operates on an hybrid HEM mode, its transfer matrix in (x, x', z, δ) is well described by the one derived in Reference [7] for a TM_{110} mode pillbox cavity with deflecting strength κ (see equation 2 in [8]); see Figure 2. Therefore this transfer matrix is used in the analytical study presented in the next Section.

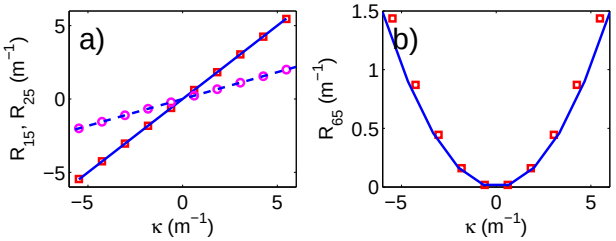

Figure 2: Comparison of the strength-dependent (κ) transfer matrix elements computed with Eq. 2 of Ref. [8] {solid (R_{25} and R_{65}) and dashed (R_{15}) lines} with the ones numerically obtained from particle tracking (symbols).

SINGLE PARTICLE DYNAMICS

Considering the single-particle dynamics in the four dimensional phase space (x, x', z, δ), an initial electron with coordinate $\widetilde{\mathbf{X_0}} \equiv (x_0, x_0', z_0, \delta_0)$ is mapped to its final coordinate $\widetilde{\mathbf{X}} \equiv (x, x', z, \delta)$ accordingly to $\mathbf{X} = R\mathbf{X_0}$ wherein R is the 4×4 transport matrix; the $\widetilde{.}$ stands for the transposition operator. The matrix associated to each subsystem have been detailed in Ref. [8]. The overall matrix of the emittance exchanger is

$$R = \begin{bmatrix} 0 & \frac{23\lambda}{128} & \mu & \eta + R_{56}\mu \\ 0 & 0 & -\frac{1}{\eta} & -\frac{R_{56}}{\eta} \\ -\frac{R_{56}}{\eta} & \eta + R_{56}\mu & \frac{23R_{56}\lambda}{128\eta^2} & \frac{23R_{56}^2\lambda}{128\eta^2} \\ -\frac{1}{\eta} & \mu & \frac{23\lambda}{128\eta^2} & \frac{\lambda R_{56}}{128\eta^2} \end{bmatrix} \quad (1)$$

where $\mu \equiv \frac{1}{\eta}(\frac{23\lambda}{128} - L - \frac{L_c}{2})$. Here R_{56} and η are respectively the longitudinal and horizontal dispersions introduced by one dogleg and λ is the free-space rf wavelength ($\lambda \simeq 0.23$ m for $f = 1.3$ GHz). The matrix R (see Eq. 1) is not block anti-diagonal yielding a non perfect emittance exchange [2, 8] and the final transverse and longitudinal emittances are respectively $\varepsilon_x = \varepsilon_{z,0}[1 + \Lambda^2 r]^{1/2}$ and $\varepsilon_z = \varepsilon_{x,0}[1 + \Lambda^2/r]^{1/2}$ where quantities with a "0" subscript correspond to the values upstream of the exchanger and $r \equiv \varepsilon_{x,0}/\varepsilon_{z,0}$. The coupling term for the beamline under consideration in this paper is

$$\Lambda^2 = \frac{529\lambda^2(1+\alpha_{x,0}^2)}{16384\eta^2\beta_{x,0}\beta_{z,0}}[R_{56}^2 + (R_{56}\alpha_{z,0} - \beta_{z,0})^2], \quad (2)$$

where $\beta_{i,0}$ and $\alpha_{i,0}$ ($i = x, z$) are the Courant-Snyder (C-S) parameters. The quantity Λ^2 is minimized for $\alpha_{z,0} = \beta_{z,0}/R_{56}$ which correspond to a chirp $d\delta/dz|_0 = -1/R_{56}$ independent of the incoming bunch length. The coupling term can in principle be further decreased by choosing $\alpha_{x0} = 0$ along with large value of $\beta_{(x,z)0}$ but these parameters are generally set from other considerations.

Particle tracking performed with ELEGANT [9] showed that when second order effects are taken into account the simple linear model fail to provide a reliable way for choosing the optimum chirp. In particular larger emittance dilutions are generally observed. To understand the underlying effect we elaborate a second order model of the emittance exchange. We use the TRANSPORT [10] formalism which describes a second order transformation via the matrix equation $X_0 \rightarrow X = RX_0 + T\Xi_0$, where T is a (4×10) matrix containing the second order map coefficient of the transformation and $\widetilde{\Xi}_0 \equiv (x_0^2, x_0x_0', x_0z_0, x_0\delta_0, {x_0'}^2, x_0'z_0, x_0'\delta_0, {z_0}^2, z_0\delta_0, {\delta_0}^2)$. Assuming a symmetric initial distribution with no coupling between the (x, x') and (z, δ) trace spaces, the final beam matrix takes the simple form

$$\langle X\widetilde{X}\rangle = R\langle X_0\widetilde{X_0}\rangle\widetilde{R} + T\langle\Xi_0\widetilde{\Xi_0}\rangle\widetilde{T}, \quad (3)$$

where the matrix $\Upsilon \equiv \langle\Xi_0\widetilde{\Xi_0}\rangle$ is a 10×10 symmetric (i.e. $\Upsilon_{i,j} = \Upsilon_{j,i}$) matrix with $\Upsilon_{1,1} = \langle x^4\rangle$, $\Upsilon_{1,4} = \Upsilon_{2,2} = \langle x^2x'^2\rangle$, $\Upsilon_{4,4} = \langle x'^4\rangle$, $\Upsilon_{8,8} = \langle z^4\rangle$, $\Upsilon_{8,10} = \Upsilon_{9,9} = \langle z^2\delta^2\rangle$, $\Upsilon_{10,10} = \langle\delta^4\rangle$ and the other elements are zeros. Taking the determinant of Eq. 3 provides the trace space emittances. The final expressions for the emittances are solved numerically to seek the optimum chirp that minimizes the coupling term. In particular we find that the optimum chirp needed to minimize the coupling term is now a function of incoming bunch length; see Fig. 3.

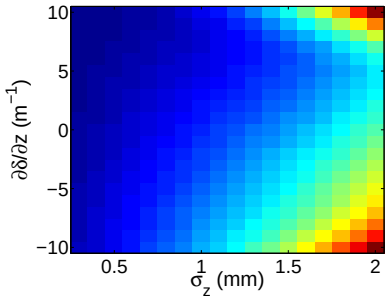

Figure 3: Optimum initial chirp $d\delta/dz|_0 = -1/R_{56}$ that minimizes horizontal emittance dilution when 2^{nd} order effects are taken into account.

COLLECTIVE EFFECTS

Detailed particle-in-cell simulations of the emittance exchange were performed with IMPACT-T [11]. Coherent synchrotron radiation has not yet been included in our simulations but simple estimates indicate space charge is the main collective effect responsible for phase space dilution at 12 MeV and with $Q = 100$ pC. All the beamline elements were modeled using realistic electromagnetic fields. The deflecting mode cavity was simulated with CSTMWS [12] and the generated 3-D field map imported in IMPACT-T. Similarly, the horizontally-bending dipoles were modeled using 8^{th}-order Enge functions. All the simulations are performed for a bunch charge of 100 pC.

In Fig. 4 we illustrate the emittance dilution dependence on incoming transverse C-S parameters. For these calculations a six-dimensional Gaussian phase space distribution is generated with its longitudinal C-S parameters and emittance partition consistent with the values obtained after optimization of the AWA accelerator [13].

The beam parameters associated to the beamline settings that realize the best emittance exchange are shown in Fig. 5. Here the distribution obtained from PIC simulation of the cathode to $z \simeq 2.8$ m was matched, using a set of four quadrupoles, to horizontal C-S parameters close to the optimum ones; see Fig. 4. The influence of space charge effects within the emittance exchanger beamline is summarized in Table 1 where the relative emittance dilution, e.g., for the horizontal (longitudinal) plane is defined as $\delta x(z) \equiv \varepsilon_{x(z)f}/\varepsilon_{z(x)0} - 1$ where the subscript f refer to the final emittances value downstream of the exchanger beamline. The intial emittance partition is $(\varepsilon_{x,0}, \varepsilon_{z,0}) = (22.30, 2.90)$ μm.

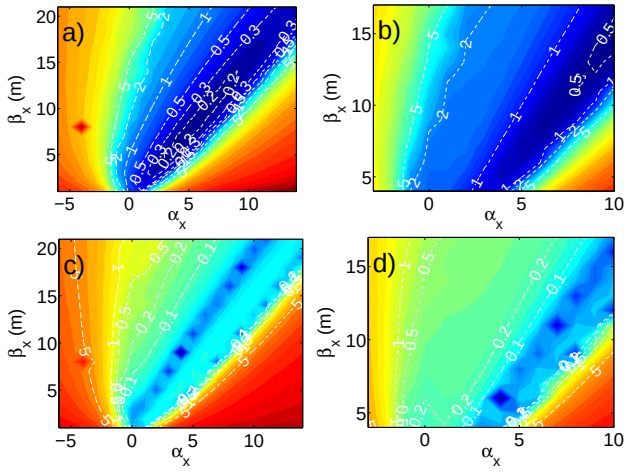

Figure 4: Transverse [plots a) and b)] and longitudinal [plots c) and d)] emittance dilution as a function of initial horizontal C-S parameters without [plots a) and c)] and with [plots b) and d)] accounting for space charge effects.

Table 1: Simulated relative emittance dilution through the exchanger beamline with and without including space charge effects.

	$\varepsilon_{zf}/\varepsilon_{x0}-1$	$\varepsilon_{xf}/\varepsilon_{z0}-1$
space charge off	1.6 %	51 %
space charge on	3.6 %	85 %

TOLERANCE & JITTER

Simulation aimed at exploring the sensitivity of the final beam parameters on the phase and field amplitude of the deflecting cavity were performed. The corresponding emittance variation compared to the nominal emittance obtained for the nominal settings $\kappa = -1/\eta$ (matching condition for emittance exchange) and $\phi = 0$ (zero-crossing) are shown in Fig. 6. Overall phase stability at the $\sim 1^\circ$ level and amplitude jitter below ~ 1 % are required to avoid significant emittance growth (< 20 %) from the ideal settings. These requirements are well within the capabilities of the AWA low-level rf system.

Surprisingly, while performing these studies, we found that operating the cavity at an amplitude slightly off its nominal settings might provide another "knob" for improving the performance of the emittance exchange. This finding will be the object of a future investigation.

REFERENCES

[1] Y. Orlov, *et al.*, Proc. PAC91 (San Francisco), 2838 (1991).

[2] M. Cornachia, *et al.*, *Phys. Rev. STAB* **6** 030702 (2003).

[3] P. Emma, *et al.*, *Phys. Rev. STAB* **9**, 100702 (2006).

[4] R. Fliller, Fermilab report BeamDocs 2271-v2 (2007).

[5] `http://gate.hep.anl.gov/awa`.

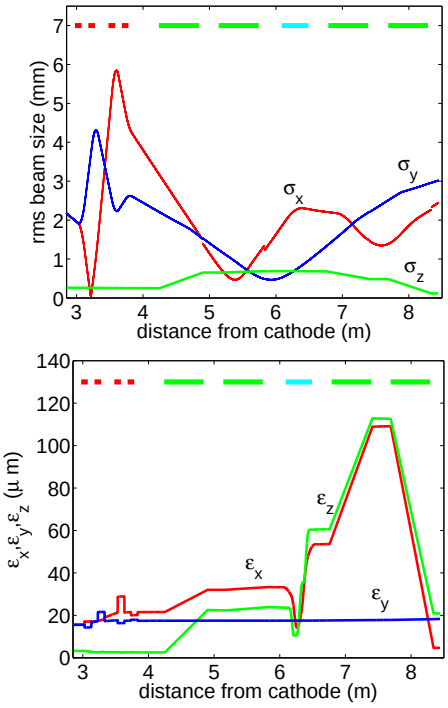

Figure 5: Evolution of horizontal (red) vertical (blue) and longitudinal (green) rms sizes (top) and trace space emittances (bottom) along the beamline shown in Fig. 1. The red, green and cyan rectangles respectively correspond to the locations of the quadrupoles, dipoles and deflecting cavity.

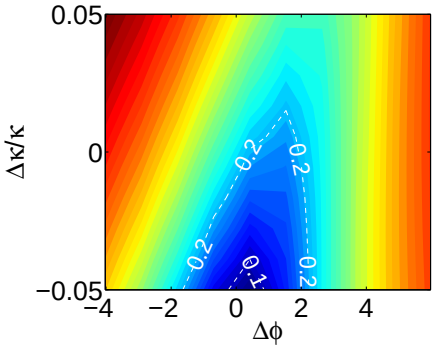

Figure 6: Relative emittance dilution with respect to the nominal setting $(\Delta\kappa/\kappa, \Delta\phi) = (0, 0)$ as a function of phase and amplitude variation of the deflecting cavity.

[6] J. Shi, *et al.* Nucl. Instr. Meth. **A 598**, 388 (2009).

[7] D. Edwards, "Notes on transit in deflecting mode pillbox cavity," (2007), unpublished.

[8] Y.-E Sun, *et al*, Proc. PAC07 (Albuquerque), 3441 (2007).

[9] M. Borland, ANL/APS, report LS-287 (2000).

[10] K. L. Brown, SLAC report SLAC-r-75 (1982).

[11] J. Qiang, *et al.*, *Phys. Rev. STAB* **9**, 044204. (2006)

[12] CSTMWS from Computer Simulation Technology AG.

[13] M. Rihaoui, *et al.*, these proceedings.